

Parrot: Pareto-optimal Multi-Reward Reinforcement Learning Framework for Text-to-Image Generation

Seung Hyun Lee^{1,6*}, Yinxiao Li¹, Junjie Ke¹, Innfarn Yoo², Han Zhang³, Jiahui Yu^{4†}, Qifei Wang², Fei Deng^{2,5*}, Glenn Entis¹, Junfeng He¹, Gang Li¹, Sangpil Kim⁶, Irfan Essa¹, Feng Yang¹
 Google Research¹, Google², Google DeepMind³, OpenAI⁴, Rutgers University⁵, Korea University⁶

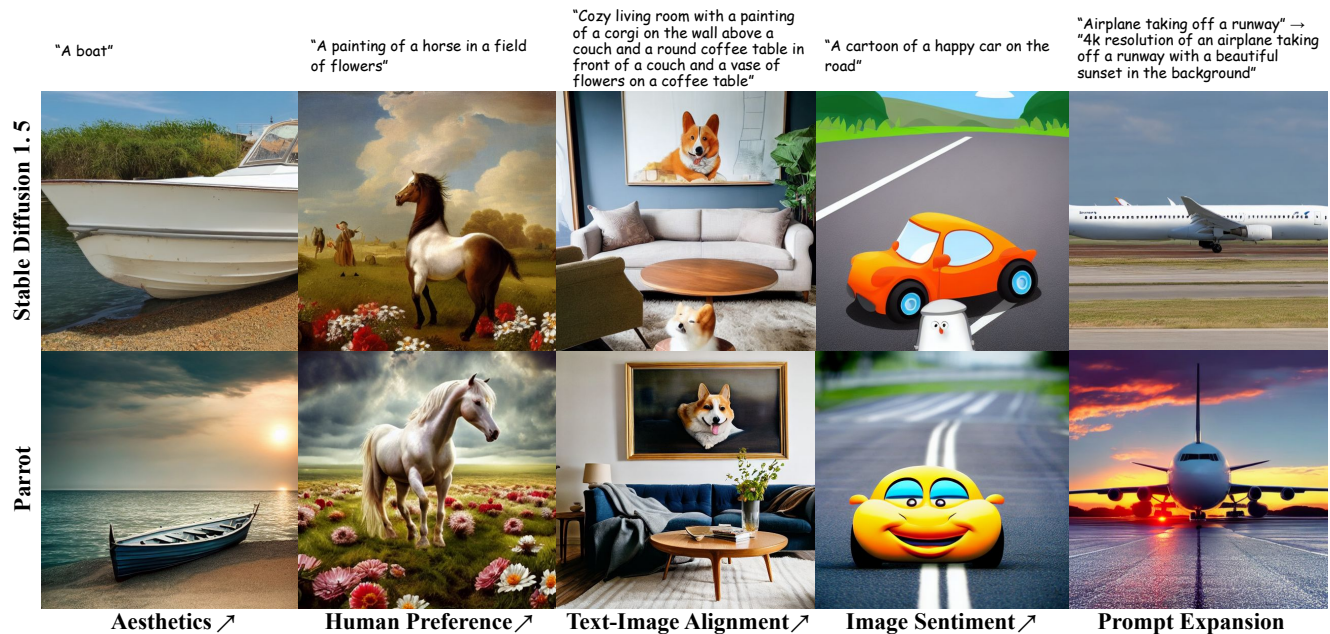


Figure 1. **Parrot visual examples.** Parrot consistently improves the quality of generated images across multiple criteria: aesthetics, human preference, text-image alignment, and image sentiment. Moreover, Parrot handles prompt expansion to complement semantics of the text input for high-quality image generation. Each column generated images using the same seed.

Abstract

Recent works demonstrate that using reinforcement learning (RL) with quality rewards can enhance the quality of generated images in text-to-image (T2I) generation. However, a simple aggregation of multiple rewards may cause over-optimization in certain metrics and degradation in others, and it is challenging to manually find the optimal weights. An effective strategy to jointly optimize multiple rewards in RL for T2I generation is highly desirable. This paper introduces Parrot, a novel multi-reward RL framework for T2I generation. Through the use of the batch-wise Pareto optimal selection, Parrot automatically identifies the optimal trade-off among different rewards during the RL optimization of the T2I generation. Additionally,

Parrot employs a joint optimization approach for the T2I model and the prompt expansion network, facilitating the generation of quality-aware text prompts, thus further enhancing the final image quality. To counteract the potential catastrophic forgetting of the original user prompt due to prompt expansion, we introduce original prompt centered guidance at inference time, ensuring that the generated image remains faithful to the user input. Extensive experiments and a user study demonstrate that Parrot outperforms several baseline methods across various quality criteria, including aesthetics, human preference, image sentiment, and text-image alignment.

1. Introduction

Recent progress in diffusion models [15, 26, 36, 45, 55] combined with pre-trained text encoders has resulted in remarkable results in text-to-image (T2I) generation. These

* This work was done during an internship at Google.

† This work was done during working at Google.

advancements have enabled the creation of high-fidelity novel images based on user-input text prompts. However, despite these advances, existing T2I models, such as Imagen [41] and Stable Diffusion [38], still generate images that fall short of the ideal. For example, the images in the first row in Fig. 1 exhibits quality issues such as poor composition (*e.g.* bad cropping), misalignment with the user input (*e.g.* missing objects), or generally less aesthetic pleasing. Consequently, achieving higher quality generated images with T2I generation remains a challenging task.

Quality of text-to-image generation is affected by multiple factors. Diverse quality metrics have been proposed to quantify each of these quality aspects. Some quality aspects are universal to images, including the aesthetics [20, 21, 31] of an image or whether the image is pleasing to look at [43]. There are also unique aspects regarding generated images, such as image-text alignment [33] and human preference [23] given the input prompt. Recent works [4, 10, 24] have demonstrated that incorporating such quality signals as a reward function can enhance the generated image quality of T2I models. In particular, DPOK [10] shows online reinforcement learning (RL) using ImageReward [51] score as a reward is able to improve T2I generated image quality. Given the aforementioned diverse criteria for the quality of generated images, it is a natural extension to incorporate multiple quality metrics in the RL fine-tuning of T2I models. While a straightforward strategy involves using a weighted sum of the reward scores [30, 37, 44, 49], this approach requires manual tuning of weights for different rewards, which is both time-consuming and resource-intensive. It is also not scalable as the number of rewards increase. Furthermore, optimizing one quality metric may inadvertently lead to degradation in others. For example, the model might generate an exceptionally good image without considering the relevance to the user provided prompt. Therefore, an effective strategy is needed to identify the optimal trade-off between different rewards in T2I generation.

To achieve this, we propose a novel **Pareto-optimal multi-reward reinforcement learning** framework for text-to-image generation, denoted as **Parrot**. Within a batch of samples produced by T2I models, each sample embodies a distinctive trade-off among various reward functions. By identifying and leveraging the set that attains the optimal trade-off (*i.e.* the Pareto-optimal set [29]) within such a training batch, Parrot effectively optimize multiple rewards simultaneously. This results in the generation of images with good aesthetics, proper image-text alignment, alignment with human preference, and an overall pleasing sentiment (Fig. 1).

The quality of generated images is significantly influenced by the text prompt input provided to the T2I model. Semantically rich prompts have been shown to produce higher quality images. As an example, simple prompts

like “A boat” often fail to generate highly detailed images. On the other hand, prompts with details, like “A green boat floating on the water with a beautiful sunset”, tend to generate higher quality images. Recognizing the difficulty of manually crafting effective prompts, Promptist [13] has been introduced to autonomously learn prompt expansion with large language models (LLM). This involves RL-tuning of the LLMs while keeping the T2I model frozen as a black box. However, since the T2I model is not tuned in collaboration with the prompt expansion network, it may struggle to adapt to the generated text inputs. In Parrot, we propose to jointly optimize the prompt expansion network and the T2I model using multiple quality rewards. This allows the prompt expansion network and T2I model to collaboratively generate higher quality images. To the best of our knowledge, we are the first to show the potential of joint optimization for prompt expansion and T2I models.

Moreover, although prompt expansion facilitates a more detailed context, there is a risk of catastrophic forgetting of the original input prompt. To address this challenge, we further introduce *original prompt-centered guidance* in Parrot during inference time, enabling the generated images to remain faithful to the original prompts while simultaneously incorporating additional details.

Our contributions can be summarized as follows:

- We present Parrot, a novel framework that enhances the generated image quality of T2I generation through multi-reward RL fine-tuning. Leveraging batch-wise Pareto-optimal selection, it efficiently optimizes the T2I model with multiple rewards, enabling collaborative improvement in aesthetics, human preference, image sentiment, and text-image alignment.
- We are the first to advocate for the joint optimization of the prompt expansion network and the T2I model. Our results demonstrate the superiority of this joint optimization compared to the individual fine-tuning of either the prompt expansion network or the T2I model.
- We propose original prompt-centered guidance as a means to prevent the catastrophic forgetting of the initial input prompt after prompt expansion. This ensures that the generated image stays true to the original prompt while adding more details.
- Extensive results and a user study show that Parrot outperforms several baseline methods across various quality criteria.

2. Related Work

T2I Generation: The goal of T2I generation is to create an image given an input text prompt. Several T2I generative models have been proposed and have demonstrated promising results [5, 7, 12, 18, 19, 25, 35, 40, 41, 54]. Notably, Stable Diffusion [38] models show impressive generation performance in T2I generation, leveraging latent text rep-

resentations from LLMs. Despite substantial progress, the images generated by those models still exhibit quality issues, such as bad cropping or misalignment with the input texts.

RL for T2I Fine-tuning: Fan *et al.* [9] pioneered the application of RL fine-tuning for T2I models, treating the denoising process as a multi-step decision making task. For human preference learning, recent works [4, 6, 10] have explored RL fine-tuning technique for T2I diffusion model, showcasing superior performance. In addition to fine-tuning the T2I model directly using RL, Promptist [13] fine-tunes the prompt expansion model by using image-text alignment scores and aesthetic scores as rewards. However, since the T2I model is not jointly fine-tuned, it may not adapt well to the following image generation tasks. Parrot proposes to jointly optimize the prompt expansion model and the T2I model using multi-reward RL.

Multi-objective Optimization: Multi-objective optimization problem involves optimizing multiple objective functions simultaneously. The scalarization technique [28, 47] formulates multi-objective problem into single-objective problems with the weighted sum of each score, which requires pre-defined weights for each objective. Rame *et al.* [34] proposed weighted averaging method to find Pareto frontier, leveraging multiple fine-tuned models. Lin *et al.* [27] proposes to learn a set model to map trade-off preference vectors to their corresponding Pareto solutions. Inspired by this, Parrot introduces a language-based preference vector constructed from task identifiers for each reward, then encoded by the text-encoder. In the context of multi-reward RL for T2I diffusion models, Promptist [13] uses a simple weighted sum of two reward scores. This approach requires manual tuning of the weights, which makes it time-consuming and hard to scale when the number of rewards increases.

Generated Image Quality: The quality assessment of images generated by T2I models involves multiple dimensions, and various metrics have been proposed. In this paper, we consider using four types of quality metrics as rewards: *aesthetics*, *human preference*, *image-text alignment*, and *image sentiment*. Aesthetics, capturing the overall visual appeal of the image, has been addressed using learning-based that leverage human ratings for aesthetics in real images [11, 16, 20, 21, 31, 48, 52]. Human preferences, rooted the concept of *learning from human feedback* [3, 32], involves gathering preferences at scale by having raters to compare different generations [23, 51]. Text-image alignment measures the extent to which the generated image aligns with the input prompt, CLIP [33] score is often employed, measuring the cosine distance of between contrastive image embedding and text embedding. Image sentiment is important for ensuring the generated image evokes positive emotions in the viewer. Serra *et al.* [43] predict av-

erage polarity of sentiments an image elicits, learning estimates for positive, neutral, and negative scores. In Parrot, we use its positive score as a reward for positive emotions.

3. Preliminary

Diffusion Probabilistic Models: Diffusion probabilistic models [15] generate the image by gradually denoising a noisy image. Specifically, given a real image \mathbf{x}_0 from the data distribution $\mathbf{x}_0 \sim q(\mathbf{x}_0)$, the forward process $q(\mathbf{x}_t|\mathbf{x}_0, c)$ of diffusion probabilistic models produce a noisy image \mathbf{x}_t , which induces a distribution $p(\mathbf{x}_0, c)$ conditioned on text prompt c . In classifier-free guidance [14], denoising model predicts noise $\bar{\epsilon}_\theta$ with a linear combination of the unconditional score estimates $\epsilon_\theta(\mathbf{x}_t, t)$ and the conditional score estimates $\epsilon_\theta(\mathbf{x}_t, t, c)$ as follows:

$$\bar{\epsilon}_\theta = w \cdot \epsilon_\theta(\mathbf{x}_t, t, c) + (1 - w) \cdot \epsilon_\theta(\mathbf{x}_t, t, \text{null}), \quad (1)$$

where t denotes diffusion time step, the null indicates a null text and w represents the guidance scale of classifier-free guidance where $w \geq 1$. Note that ϵ_θ is typically parameterized by the UNet [39].

RL-based T2I Diffusion Model Fine-tuning: Given a reward signal from generated images, the goal of RL-tuning for T2I diffusion models is to optimize the policy defined as one denoising step of T2I diffusion models. In particular, Black *et al.* [4] apply policy gradient algorithm, which regards the denoising process of diffusion models as a Markov decision process (MDP) by performing multiple denoising steps iteratively. Subsequently, a black box reward model $r(\cdot, \cdot)$ predicts a single scalar value from sampled image \mathbf{x}_0 . Given text condition $c \sim p(c)$ and image \mathbf{x}_0 , objective function \mathcal{J} can be defined to maximize the expected reward as follows:

$$\mathcal{J}_\theta = \mathbb{E}_{p(c)} \mathbb{E}_{p_\theta(\mathbf{x}_0|c)} [r(\mathbf{x}_0, c)], \quad (2)$$

where the pre-trained diffusion model p_θ produces a sample distribution $p_\theta(\mathbf{x}_0|c)$ using text condition c . Modifying this equation, Lee *et al.* [10] demonstrate that the gradient of objective function $\nabla \mathcal{J}_\theta$ can be calculated through gradient ascent algorithm without using the gradient of reward model as follows:

$$\nabla \mathcal{J}_\theta = \mathbb{E}[r(\mathbf{x}_0, c) \sum_{t=1}^T \nabla_\theta \log p_\theta(\mathbf{x}_{t-1}|c, t, \mathbf{x}_t)], \quad (3)$$

where T denotes the total time step of the diffusion sampling process. With parameters θ , the expectation value can be taken over trajectories of the diffusion sampling process.

4. Method

4.1. Parrot Overview

Fig. 2 shows the overview of Parrot, which consists of the prompt expansion network (PEN) p_ϕ and the T2I diffusion model p_θ . The PEN is first initialized from a supervised

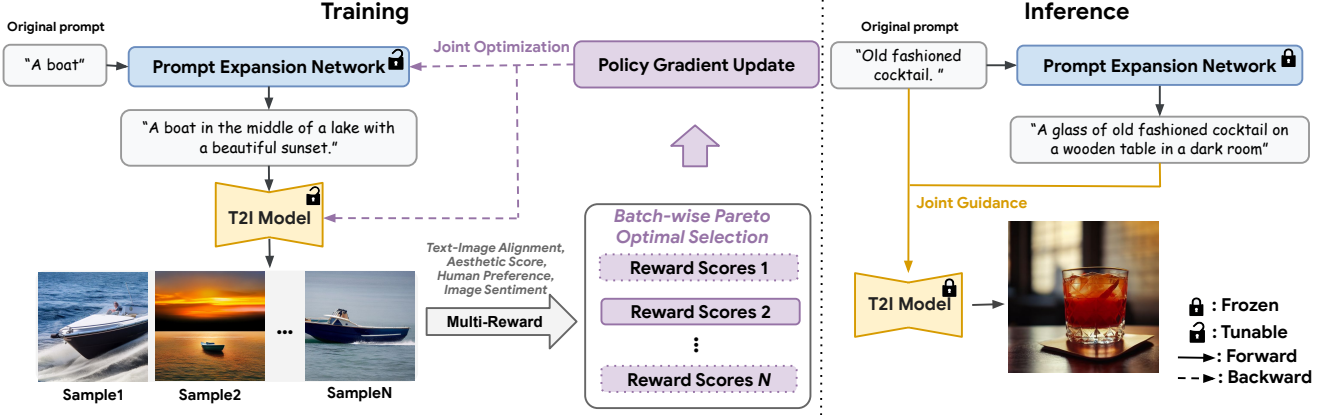


Figure 2. Overview of the **Parrot** framework. During the training, N images are generated from the T2I model using the expanded prompt from the prompt expansion network. Multiple quality rewards are calculated for each image, and the Pareto-optimal set is identified using the non-dominated sorting algorithm. These optimal images are then used to perform policy gradient update of the parameters of T2I diffusion and prompt expansion network jointly. During the inference, both the original prompt and the expanded prompt are provided to the T2I model, enabling a trade-off between faithfulness and detail.

fine-tuning checkpoint on demonstrations of prompt expansion pairs, and the T2I model is initialized from pretrained diffusion model. Given the original prompt c , the PEN generates an expanded prompt \hat{c} , and the T2I model generates images based on this expanded prompt. During the multi-reward RL fine-tuning, a batch of N images is sampled, and multiple quality rewards are calculated for each image, encompassing aspects like text-image alignment, aesthetics, human preference, and image sentiment. Based on these reward scores, Parrot identifies the batch-wise Pareto-optimal set using a non-dominated sorting algorithm. This optimal set of images is then used for joint optimization of the PEN and T2I model parameters through RL policy gradient update. During inference, Parrot leverages both the original prompt and its expansion, striking a balance between maintaining faithfulness to the original prompt and incorporating additional details for higher quality.

4.2. Batch-wise Pareto-optimal Selection

Algorithm 1 outlines the procedure of Parrot. Rather than updating the gradients using all images, Parrot focuses on high-quality samples, considering multiple quality rewards in each mini-batch. In the multi-reward RL, each sample generated by the T2I model presents distinct trade-offs for each reward. Among these samples, a subset with varied optimal trade-offs across objectives, known as the Pareto set, exists. For a Pareto-optimal sample, none of its objective values can be further improved without damaging others. In other words, the Pareto-optimal set is not dominated by any data points, also known as *the non-dominated set*. To achieve a Pareto-optimal solution with T2I diffusion model, Parrot selectively uses data points from the non-dominated set using non-dominated sorting algorithm. This naturally encourages the T2I model to produce Pareto-optimal samples with respect to the multi-reward objectives.

Reward-specific Preference: Inspired by the use of preference information in multi-objective optimization [27], Parrot incorporates the preference information through reward-specific identifiers. This enables Parrot to automatically determine the importance for each reward objective. Concretely, we enrich the expanded prompt \hat{c} by prepending reward-specific identifier “<reward k >” for k -th reward. Based on this reward-specific prompt, N images are generated and are used for maximizing the corresponding k -th reward model during gradient update. At inference time, a concatenation of all the reward identifiers “<reward 1>, ..., <reward K >” is used for image generation.

Non-dominated Sorting: Parrot constructs Pareto set with non-dominated points based on trade-offs among multiple rewards. These non-dominated points are superior to the remaining solutions and are not dominated by each other. Formally, the dominance relationship is defined as follows: the image \mathbf{x}_0^a dominates the image \mathbf{x}_0^b , denoted as $\mathbf{x}_0^a < \mathbf{x}_0^b$, if and only if $R_i(\mathbf{x}_0^b) \leq R_i(\mathbf{x}_0^a)$ for all $i \in 1, \dots, m$, and there exists $j \in 1, \dots, m$ such that $R_j(\mathbf{x}_0^a) < R_j(\mathbf{x}_0^b)$. For example, given the i -th generated image \mathbf{x}_0^i in a mini-batch, when no point in the mini-batch dominates \mathbf{x}_0^i , it is referred to as a non-dominated point.

Policy Gradient Update: We assign a reward value of zero to the data points not included in non-dominated sets and only update the gradient of these non-dominated data points as follows:

$$\nabla \mathcal{J}_\theta = \frac{1}{n(\mathcal{P})} \sum_{i=1, \mathbf{x}_0^i \in \mathcal{P}} \sum_{k=1}^K \sum_{t=1}^T r_k(\mathbf{x}_0^i, c_k) \times \nabla_\theta \log p_\theta(\mathbf{x}_{t-1}^i | c_k, t, \mathbf{x}_t^i), \quad (4)$$

where i indicates the index of images in mini-batches, and \mathcal{P} denotes batch-wise a set of non-dominated points. K and

Algorithm 1 Parrot: Pareto-optimal Multi-Reward RL

Input: Text prompt c , Batch size N , Total iteration E , the number of rewards: K , Prompt expansion network p_ϕ , T2I diffusion model: p_θ , Total diffusion time step T , Non-dominated set: \mathcal{P}

for $e = 1$ to E **do**

 Sample text prompt $c \sim p(c)$

for $k = 1$ to K **do**

 Expand text prompt $\hat{c} \sim p_\phi(\hat{c}|c)$

 Prepend reward-specific tokens “<reward k >” to \hat{c}

 Sample a set of images $\{\mathbf{x}_0^1, \dots, \mathbf{x}_0^N\} \sim p_\theta(x_0|\hat{c})$

 A set of reward vector $\mathcal{R} = \{R_1, \dots, R_N\}$

$\mathcal{P} \leftarrow \text{NONDOMINATEDSET}(\{\mathbf{x}_0^1, \dots, \mathbf{x}_0^N\})$

for j in \mathcal{P} **do**

$\nabla \mathcal{J}_\theta += \sum_{i=1}^T r_k(\mathbf{x}_0^j, \hat{c}) \cdot \nabla \log p_\theta(x_{t-1}^j | c_k, t, x_t^j)$

$\nabla \mathcal{J}_\phi += -r_k(\mathbf{x}_0^j, \hat{c}) \times \nabla \log p_\phi(\hat{c}|c)$

 Update the gradient p_θ from Eq. 4

 Update the gradient p_ϕ

Output: Fine-tuned diffusion model p_θ ,
prompt expansion network p_ϕ

function NONDOMINATEDSET($\{\mathbf{x}_0^1, \dots, \mathbf{x}_0^N\}$)

$\mathcal{P} \leftarrow \emptyset$

for $i = 1$ to N **do**

 dominance \leftarrow True

for $j = 1$ to N **do**

if \mathbf{x}_0^j dominates \mathbf{x}_0^i **then**

 dominance \leftarrow False

if dominance is True **then**

 Add i to \mathcal{P}

return \mathcal{P}

T are the total number of reward models and total diffusion time steps, respectively. The same text prompt is used when updating the diffusion model in each batch.

4.3. Original Prompt Centered Guidance

While prompt expansion enhances details and often improves generation quality, there is a concern that the added context may dilute the main content of the original input. To mitigate this during the inference, we introduce original prompt-centered guidance. When sampling conditioned on the original prompt, the diffusion model ϵ_θ typically predicts noises by combining the unconditioned score estimate and the prompt-conditioned estimate. Instead of relying solely on the expanded prompt from PEN, we propose using a linear combination of two guidances for T2I generation: one from the user input and the other from the expanded prompt. The strength of the original prompt is controlled by guidance scales w_1 and w_2 . The noise $\bar{\epsilon}_\theta$ is estimated, derived from Eq. 1, as follows:

$$\bar{\epsilon}_\theta = w_1 \cdot \epsilon_\theta(\mathbf{x}_t, t, c) + (1 - w_1) \cdot \epsilon_\theta(\mathbf{x}_t, t, \text{null}) + \quad (5)$$

$$w_2 \cdot \epsilon_\theta(\mathbf{x}_t, t, \hat{c}) + (1 - w_2) \cdot \epsilon_\theta(\mathbf{x}_t, t, \text{null}), \quad (6)$$

where null denotes a null text.

5. Experiments

5.1. Experiment Setting

Dataset: The PEN is first supervised fine-tuned on a large-scale text dataset named the Promptist [13], which has 360K constructed prompt pairs for original prompt and prompt expansion demonstration. The original instruction “*Rephrase*” is included per pair in Promptist. We modify the instruction into “*Input: <original prompt>. This is a text input for image generation. Expand prompt for improving image quality. Output:* ”. Subsequently, we use the RL tuning prompts (1200K) from Promptist for RL training of the PEN and T2I model.

T2I Model: Our T2I model is based on the JAX version of Stable Diffusion 1.5 [38] pre-trained with the LAION-5B [42] dataset. We conduct experiments on a machine equipped with 16 NVIDIA RTX A100 GPUs. DDIM [46] with 50 denoising steps is used, and the classifier-free guidance weight is set to 5.0 with the resolution 512×512. Instead of updating all layers, we specifically update the cross-attention layer in the Denoising U-Net. For optimization, we employ the Adam [22] optimizer with a learning rate of 1×10^{-5} .

Prompt Expansion Network: For prompt expansion, we use PaLM 2-L-IT [2], one of the PaLM2 variations, which is a multi-layer Transformer [50] decoder with causal language modeling. We optimize LoRA [17] weights for RL-based fine-tuning. The output token length of the PEN is set to 77 to match the maximum number of token length for Stable Diffusion. For original prompt-centered guidance, we set both w_1 and w_2 to 5 in Eq. 6.

Reward Models: We incorporate four quality signals as rewards: *Aesthetics*, *Human preference*, *Text-Image Alignment*, *Image Sentiment*. For aesthetics, we use the VILA-R [21] pre-trained with the AVA [31] dataset. For human preference, we train a ViT-B/16 [8] using the Pick-a-Pic [23] dataset, which contains 500K examples for human feedback in T2I generation. The ViT-B/16 image encoder consists of 12 transformer layers, and the image resolution is 224×224 with a patch size of 16×16. For text-image alignment, we use CLIP [33] with the image encoder ViT-B/32. For image sentiment, we use the pre-trained model from [43], which outputs three labels: positive, neutral, negative. We use the positive score ranging from 0 to 1 as the sentiment reward.

5.2. Qualitative Analysis

Comparison with Baselines: Fig 3 shows the visual comparison of Parrot and multiple baselines. We include results from Stable Diffusion 1.5, DPOK [10] with a weighted sum of rewards, Promptist [13], and Parrot. DPOK exclusively fine-tunes the T2I model, while Promptist focuses on fine-tuning only the prompt expansion network. Parrot shows vi-

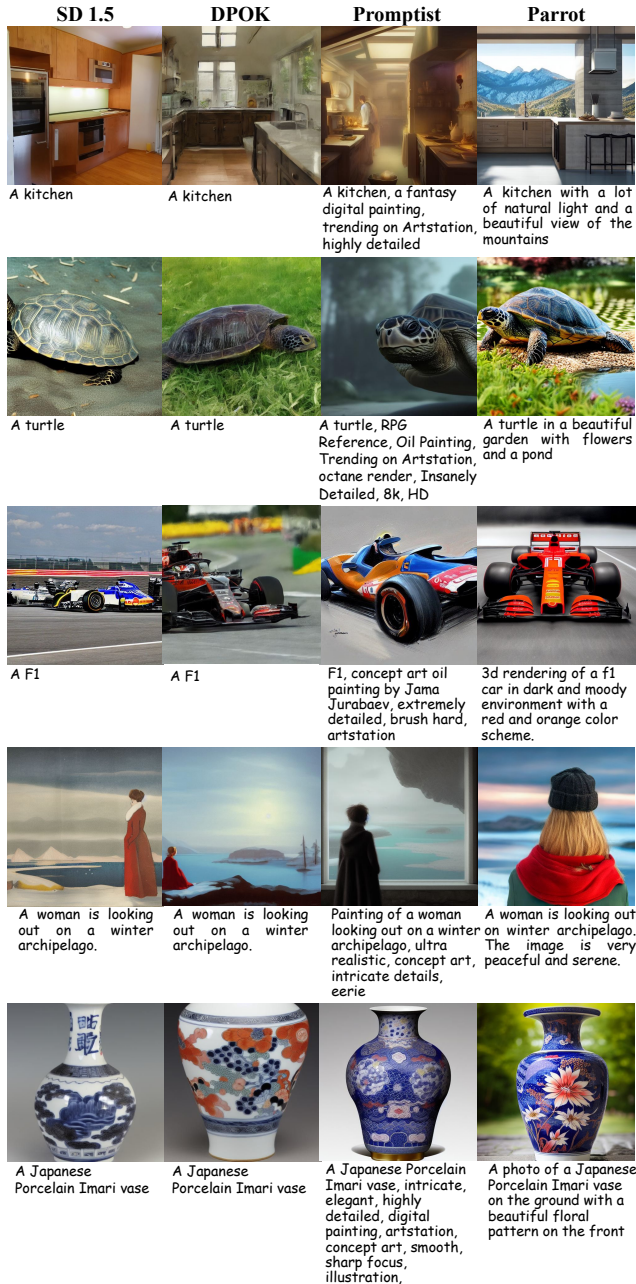


Figure 3. **Comparison of Parrot and diffusion-based RL baselines.** From left to right, we provide results of Stable diffusion 1.5 [38] (1st column), DPOK [10] (2nd column) with the weighted sum, the Promptist [13] (3rd column), and the Parrot (4th column).

usually better images, particularly in aspects like color combination, cropping, perspective, and fine details in the image. This improvement can be attributed to Parrot’s T2I model being fine-tuned together with the prompt expansion model that incorporates aesthetic keywords during training. Parrot generates results that are more closely aligned with the input prompt, as well as more visually pleasing.

Fig. 4 shows the training curve comparison of Parrot and

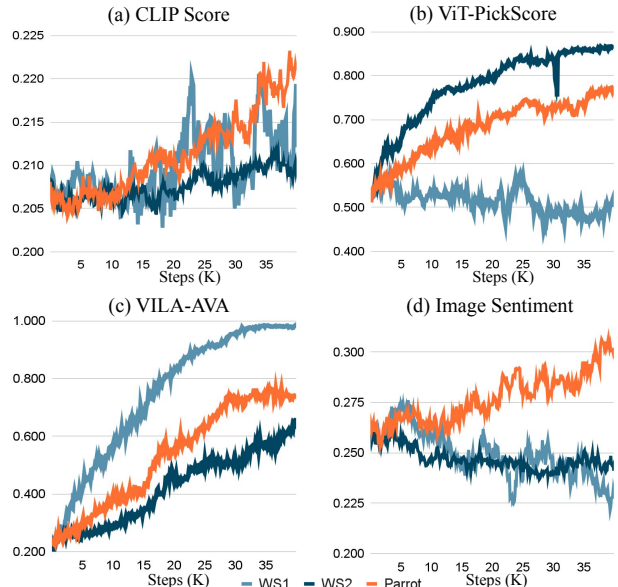


Figure 4. **Training curve for fine-tuning on weighted sum and Parrot.** For weighted sum, WS1 denotes $\{0.7, 0.1, 0.1, 0.1\}$ and WS2 denotes $\{0.25, 0.25, 0.25, 0.25\}$ for aesthetics, human preference, text-image alignment and image sentiment. Using weighted sum leads to decrease in human preference score and image sentiment score despite an improvement in the aesthetic score. In contrast, Parrot exhibits stable increases across all metrics.

Model	Quality Metrics			
	TIA (\uparrow)	Aesth (\uparrow)	HP (\uparrow)	IS (\uparrow)
SD 1.5 [38]	0.2322	0.5755	0.1930	0.3010
DPOK [10] (WS)	0.2337	0.5813	0.1932	0.3013
Parrot w/o PE	0.2355	0.6034	0.2009	0.3018
Promptist [13]	0.1449	0.6783	0.2759	0.2518
Parrot	0.1667	0.7396	0.3411	0.3132

Table 1. Quantitative comparison between Parrot and alternatives on the Parti dataset [53]. Abbreviations: WS - Weighted Sum; PE - Prompt Expansion; TIA - Text-Image Alignment; Aesth - Aesthetics; HP - Human Preference; IS - Image Sentiment. TIA score is measured against the original prompt without expansion.

using a linear combination of the reward scores. Each subgraph represents a reward. WS1 and WS2 denote two different weights with multiple reward scores. WS1 places greater emphasis on the aesthetic score, while WS2 adopts balanced weights across aesthetics, human preference, text-image alignment, and image sentiment. Employing the weighted sum of multiple rewards leads to a decrease in the image sentiment score, despite notable enhancements in aesthetics and human preference. In contrast, Parrot consistently exhibits improvement across all metrics.

5.3. Quantitative Evaluation

Comparison with Baselines: Table 1 presents our results of the quality score across four quality rewards: text-image alignment score, aesthetic score, human preference score,

Area	Question
Aesthetics	“Which image shows better aesthetics without blurry texture, unnatural focusing, and poor color combination?”
Human Preference	“Which generated image do you prefer?”
Text-Image Alignment	“Which image is well aligned with the text?”
Image Sentiment	“Which image is closer to amusement, excitement, and contentment?”

Table 2. Questions for user study. For performing user study, we carefully design questions suitable to each quality.

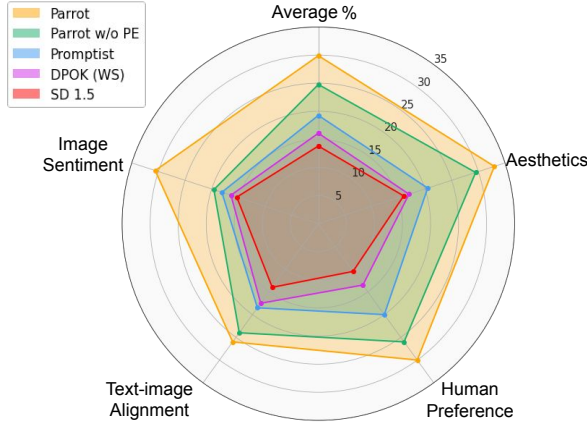


Figure 5. User study results on PartiPrompts [53]. Parrot outperforms baselines across all metrics.

and emotion score. The first group shows methods without prompt expansion, and the second group compares methods with expansion. The prompt expansion and T2I generation are performed on the PartiPrompts [53]. Using a set of 1631 prompts, we generate 32 images for each text input and calculate the average for each metric. “w/o Prompt Expansion” indicates the generation of images solely based on original prompt without expansion. We compare with DPOK [10] with a weighted sum (WS) of rewards, using balanced weights of $\{0.25, 0.25, 0.25, 0.25\}$. For Promptist [13], we generate prompt expansion from their model. Our method outperforms both compared methods in aesthetics, human preference and sentiment scores. The text-image alignment score is measured with the original prompt before expansion for fair comparison. As a result, the group without prompt expansion generally shows a higher text-image alignment score. Parrot shows better text-image alignment in each subgroup.

User Study: We conduct a user study using MTurk [1] with generated images from 100 random prompts in the PartiPrompts [53]. Five models are compared: Stable Diffusion v1.5, DPOK [10] with an equal weighted sum, Promptist [13], Parrot without prompt expansion, and Parrot. Each rater is presented with the original prompt (before expansion) and a set of five generated images, with the image order being randomized. Raters are then tasked with selecting



Figure 6. **Ablation study.** We perform an ablation study by removing one of quality signals. We observe that each quality signal affects their improvement of (a) aesthetics, (b) human preference score, (c) text-image alignment score, (d) image sentiment score.

the best image from the group, guided by questions outlined in Table 2. Each question pertains to a specific quality aspect: aesthetics, human preference, text-image alignment, and image sentiment. For each prompt, 20 rounds of random sampling are conducted and sent to different raters. The aggregated user study results, illustrated in Fig 5, show that Parrot significantly outperforms other baselines across all dimensions.

5.4. Ablations

Effect of Pareto-optimal Multi-reward RL: To show the efficacy of Pareto-optimal Multi-reward RL, we conduct an ablation study by removing one reward model at a time. Fig 6 shows quantitative results using one hundred random text prompts from the Promptist [13]. We observe that our training scheme improves multiple target objectives. Fig 7 shows the visual comparison between Parrot, Parrot with a single reward, and Parrot without selecting the batch-wise Pareto-optimal solution. Using a single reward model tends to result in degradation of another reward, especially text-image alignment. For example, in the third column, results of the first row miss the prompt *a tophat*, even though the Stable Diffusion result includes that attribute. On the other hand, Parrot results capture all prompts, improving other quality signals, such as aesthetics, image sentiment and human preference.

Effect of Original Prompt Centered Guidance: Fig 8 shows the effect of the proposed original prompt-centered guidance. As evident from the figure, utilizing only the expanded prompt as input often results in the main content being overwhelmed by the added context. For instance, given the original prompt “A shiba inu”, the result from the expanded prompt shows a zoomed-out image and the intended main subject (shiba inu) becomes small. The proposed original prompt-centered guidance effectively addresses this issue, generating an image that faithfully captures the original prompt while incorporating visually more pleasing details.

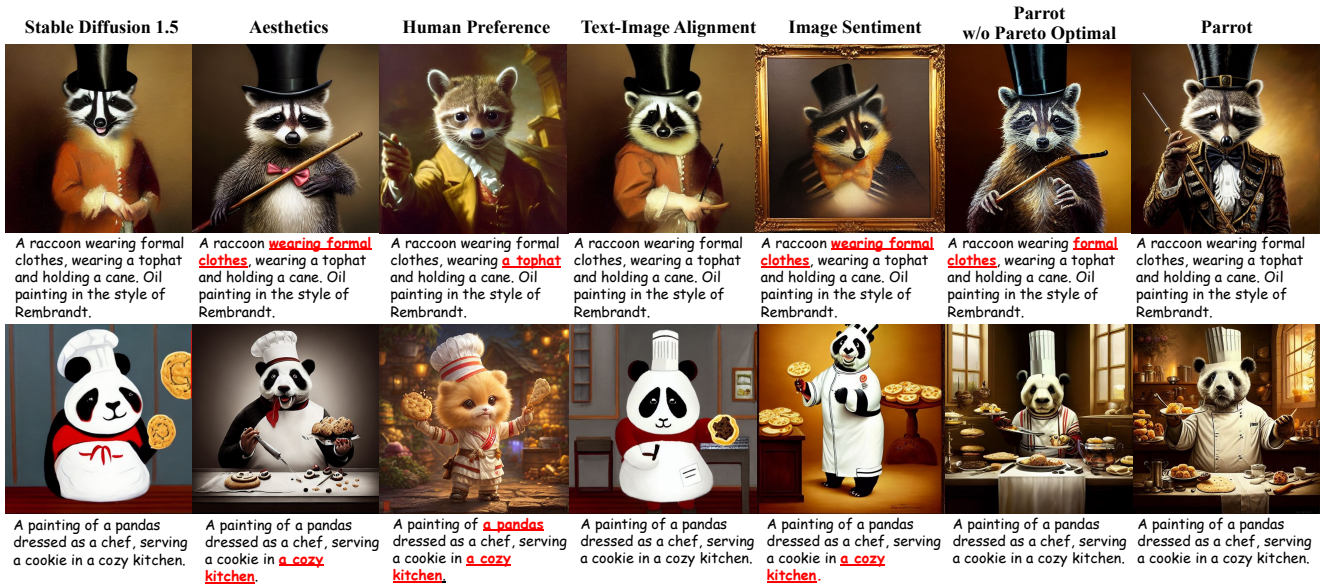


Figure 7. The comparisons of the diffusion fine-tuning between Pareto-optimal multi-reward RL and single reward RL. We show results with same seed from various methods: Stable Diffusion 1.5 [38] (1st column), T2I model fine-tuned with the aesthetic model (2nd column), the human preference model (3rd column), text-image alignment (4th column), image sentiment (5th column), Parrot without Pareto-optimal selection (6th column) and Parrot (7th column). Parrot is effective to generate acceptable images without sacrificing one of quality signals. For example, T2I model fine-tuned with a single quality signal such as aesthetics, human preference and image sentiment results in text-image misalignment. In contrast, our method achieves a balanced visual outcome across multiple criteria.



Figure 8. Results of original prompt centered guidance. As we expand the prompt, the content in the generated image often fades away (2nd column). We observe that this guidance is helpful for keeping the main content of the original prompt.

6. Conclusion and Limitation

In this paper, we propose Parrot, a framework designed to improve T2I generation by effectively optimizing multiple quality rewards using RL. With batch-wise Pareto-optimal selection, we effectively balance the optimization process of multiple quality rewards, improving each quality metric. Furthermore, through co-training the T2I model and the prompt expansion model, Parrot can generate higher-quality images. Additionally, our original prompt centered guidance technique enables the control over the persistence of the main content in user input, ensuring that the generated image remains faithful to the user prompt. Results from the user study indicate that Parrot significantly elevates the quality of generated images across multiple criteria including text-image alignment, human preference, aesthetics, and image sentiment. While Parrot has demonstrated effectiveness in enhancing generated image quality, its efficacy is limited by the quality metrics it relies on. Consequently, advancements of the generated image quality metrics will directly enhance the capabilities of Parrot. Additionally, Parrot is adaptable to a broader range of rewards that quantify generated image quality.

Societal Impact: Parrot could potentially raise ethical concerns related to the generation of immoral content. This concern stems from the user’s ability to influence T2I generation, allowing for the creation of visual content that may be deemed inappropriate. The risk may be tied to the potential biases in reward models inherited from various datasets.

References

- [1] Amazon mechanical turk. <https://www.mturk.com/>, 2005. 7
- [2] Rohan Anil, Andrew M Dai, Orhan Firat, Melvin Johnson, Dmitry Lepikhin, Alexandre Passos, Siamak Shakeri, Emanuel Taropa, Paige Bailey, Zhifeng Chen, et al. Palm 2 technical report. *arXiv preprint arXiv:2305.10403*, 2023. 5
- [3] Yuntao Bai, Andy Jones, Kamal Ndousse, Amanda Askell, Anna Chen, Nova DasSarma, Dawn Drain, Stanislav Fort, Deep Ganguli, Tom Henighan, et al. Training a helpful and harmless assistant with reinforcement learning from human feedback. *arXiv preprint arXiv:2204.05862*, 2022. 3
- [4] Kevin Black, Michael Janner, Yilun Du, Ilya Kostrikov, and Sergey Levine. Training diffusion models with reinforcement learning. In *ICML Workshop*, 2023. 2, 3, 1
- [5] Huiwen Chang, Han Zhang, Jarred Barber, AJ Maschinot, Jose Lezama, Lu Jiang, Ming-Hsuan Yang, Kevin Murphy, William T Freeman, Michael Rubinstein, et al. Muse: Text-to-image generation via masked generative transformers. In *ICML*, 2023. 2
- [6] Kevin Clark, Paul Vicol, Kevin Swersky, and David J Fleet. Directly fine-tuning diffusion models on differentiable rewards. *arXiv preprint arXiv:2309.17400*, 2023. 3
- [7] Xiaoliang Dai, Ji Hou, Chih-Yao Ma, Sam Tsai, Jialiang Wang, Rui Wang, Peizhao Zhang, Simon Vandenhende, Xiaofang Wang, Abhimanyu Dubey, et al. Emu: Enhancing image generation models using photogenic needles in a haystack. *arXiv preprint arXiv:2309.15807*, 2023. 2
- [8] Alexey Dosovitskiy, Lucas Beyer, Alexander Kolesnikov, Dirk Weissenborn, Xiaohua Zhai, Thomas Unterthiner, Mostafa Dehghani, Matthias Minderer, Georg Heigold, Sylvain Gelly, et al. An image is worth 16x16 words: Transformers for image recognition at scale. In *ICLR*, 2021. 5
- [9] Ying Fan and Kangwook Lee. Optimizing ddpm sampling with shortcut fine-tuning. In *ICML*, 2023. 3, 1, 7, 8
- [10] Ying Fan, Olivia Watkins, Yuqing Du, Hao Liu, Moonkyung Ryu, Craig Boutilier, Pieter Abbeel, Mohammad Ghavamzadeh, Kangwook Lee, and Kimin Lee. Dpoc: Reinforcement learning for fine-tuning text-to-image diffusion models. In *NeurIPS*, 2023. 2, 3, 5, 6, 7, 1, 8
- [11] Yuming Fang, Hanwei Zhu, Yan Zeng, Kede Ma, and Zhou Wang. Perceptual quality assessment of smartphone photography. In *CVPR*, 2020. 3
- [12] Ligong Han, Yinxiao Li, Han Zhang, Peyman Milanfar, Dimitris Metaxas, and Feng Yang. Svdiff: Compact parameter space for diffusion fine-tuning. In *ICCV*, 2023. 2
- [13] Yaru Hao, Zewen Chi, Li Dong, and Furu Wei. Optimizing prompts for text-to-image generation. In *CoRR*, 2022. 2, 3, 5, 6, 7
- [14] Jonathan Ho and Tim Salimans. Classifier-free diffusion guidance. In *CoRR*, 2022. 3
- [15] Jonathan Ho, Ajay Jain, and Pieter Abbeel. Denoising diffusion probabilistic models. In *NeurIPS*, 2020. 1, 3
- [16] Vlad Hosu, Hanhe Lin, Tamas Sziranyi, and Dietmar Saupe. Koniq-10k: An ecologically valid database for deep learning of blind image quality assessment. *TIP*, 29:4041–4056, 2020. 3
- [17] Edward J Hu, Yelong Shen, Phillip Wallis, Zeyuan Allen-Zhu, Yuanzhi Li, Shean Wang, Lu Wang, and Weizhu Chen. Lora: Low-rank adaptation of large language models. 2022. 5
- [18] Yujin Jeong, Wonjeong Ryoo, Seunghyun Lee, Dabin Seo, Wonmin Byeon, Sangpil Kim, and Jinkyu Kim. The power of sound (tpos): Audio reactive video generation with stable diffusion. In *ICCV*, 2023. 2
- [19] Bahjat Kawar, Shiran Zada, Oran Lang, Omer Tov, Huiwen Chang, Tali Dekel, Inbar Mosseri, and Michal Irani. Imagic: Text-based real image editing with diffusion models. In *CVPR*, 2023. 2
- [20] Junjie Ke, Qifei Wang, Yilin Wang, Peyman Milanfar, and Feng Yang. Musiq: Multi-scale image quality transformer. In *ICCV*, 2021. 2, 3
- [21] Junjie Ke, Keren Ye, Jiahui Yu, Yonghui Wu, Peyman Milanfar, and Feng Yang. Vila: Learning image aesthetics from user comments with vision-language pretraining. In *CVPR*, 2023. 2, 3, 5
- [22] Diederik P Kingma and Jimmy Ba. Adam: A method for stochastic optimization. In *ICLR*, 2015. 5, 1
- [23] Yuval Kirstain, Adam Polyak, Uriel Singer, Shahbuland Matiana, Joe Penna, and Omer Levy. Pick-a-pic: An open dataset of user preferences for text-to-image generation. 2023. 2, 3, 5
- [24] Kimin Lee, Hao Liu, Moonkyung Ryu, Olivia Watkins, Yuqing Du, Craig Boutilier, Pieter Abbeel, Mohammad Ghavamzadeh, and Shixiang Shane Gu. Aligning text-to-image models using human feedback. In *CoRR*, 2023. 2
- [25] Seung Hyun Lee, Sieun Kim, Innfarn Yoo, Feng Yang, Donghyeon Cho, Youngseo Kim, Huiwen Chang, Jinkyu Kim, and Sangpil Kim. Soundini: Sound-guided diffusion for natural video editing. *arXiv preprint arXiv:2304.06818*, 2023. 2
- [26] Yuheng Li, Haotian Liu, Qingyang Wu, Fangzhou Mu, Jianwei Yang, Jianfeng Gao, Chunyuan Li, and Yong Jae Lee. Gligen: Open-set grounded text-to-image generation. In *CVPR*, 2023. 1
- [27] Xi Lin, Zhiyuan Yang, Xiaoyuan Zhang, and Qingfu Zhang. Pareto set learning for expensive multi-objective optimization. In *NeurIPS*, 2022. 3, 4
- [28] Shie Mannor and Nahum Shimkin. The steering approach for multi-criteria reinforcement learning. In *NeurIPS*, 2001. 3
- [29] Kaisa Miettinen. *Nonlinear multiobjective optimization*. Springer Science & Business Media, 1999. 2
- [30] Hossam Mossalam, Yannis M Assael, Diederik M Roijers, and Shimon Whiteson. Multi-objective deep reinforcement learning. In *CoRR*, 2016. 2
- [31] Naila Murray, Luca Marchesotti, and Florent Perronnin. Ava: A large-scale database for aesthetic visual analysis. In *CVPR*, 2012. 2, 3, 5
- [32] Long Ouyang, Jeffrey Wu, Xu Jiang, Diogo Almeida, Carroll Wainwright, Pamela Mishkin, Chong Zhang, Sandhini Agarwal, Katarina Slama, Alex Ray, et al. Training language models to follow instructions with human feedback. In *NeurIPS*, 2022. 3

- [33] Alec Radford, Jong Wook Kim, Chris Hallacy, Aditya Ramesh, Gabriel Goh, Sandhini Agarwal, Girish Sastry, Amanda Askell, Pamela Mishkin, Jack Clark, et al. Learning transferable visual models from natural language supervision. In *ICML*, 2021. 2, 3, 5
- [34] Alexandre Rame, Guillaume Couairon, Mustafa Shukor, Corentin Dancette, Jean-Baptiste Gaya, Laure Soulier, and Matthieu Cord. Rewarded soups: towards pareto-optimal alignment by interpolating weights fine-tuned on diverse rewards. In *NeurIPS*, 2023. 3
- [35] Aditya Ramesh, Prafulla Dhariwal, Alex Nichol, Casey Chu, and Mark Chen. Hierarchical text-conditional image generation with clip latents. *arXiv preprint arXiv:2204.06125*, 2022. 2
- [36] Elad Richardson, Kfir Goldberg, Yuval Alaluf, and Daniel Cohen-Or. Conceptlab: Creative generation using diffusion prior constraints. *arXiv preprint arXiv:2308.02669*, 2023. 1
- [37] Diederik M Roijers, Peter Vamplew, Shimon Whiteson, and Richard Dazeley. A survey of multi-objective sequential decision-making. *JAIR*, 48:67–113, 2013. 2
- [38] Robin Rombach, Andreas Blattmann, Dominik Lorenz, Patrick Esser, and Björn Ommer. High-resolution image synthesis with latent diffusion models. In *CVPR*, 2022. 2, 5, 6, 8, 1, 4, 7
- [39] Olaf Ronneberger, Philipp Fischer, and Thomas Brox. U-net: Convolutional networks for biomedical image segmentation. In *MICCAI*, 2015. 3
- [40] Chitwan Saharia, William Chan, Huiwen Chang, Chris Lee, Jonathan Ho, Tim Salimans, David Fleet, and Mohammad Norouzi. Palette: Image-to-image diffusion models. In *SIGGRAPH*, 2022. 2
- [41] Chitwan Saharia, William Chan, Saurabh Saxena, Lala Li, Jay Whang, Emily L Denton, Kamyar Ghasemipour, Raphael Gontijo Lopes, Burcu Karagol Ayan, Tim Salimans, et al. Photorealistic text-to-image diffusion models with deep language understanding. In *NeurIPS*, 2022. 2
- [42] Christoph Schuhmann, Romain Beaumont, Richard Vencu, Cade Gordon, Ross Wightman, Mehdi Cherti, Theo Coombes, Aarush Katta, Clayton Mullis, Mitchell Wortsman, et al. Laion-5b: An open large-scale dataset for training next generation image-text models. *NeurIPS*, 2022. 5
- [43] Alessio Serra, Fabio Carrara, Maurizio Tesconi, and Fabrizio Falchi. The emotions of the crowd: Learning image sentiment from tweets via cross-modal distillation. *ECAI*, 2023. 2, 3, 5
- [44] Christian Shelton. Balancing multiple sources of reward in reinforcement learning. In *NeurIPS*, 2000. 2
- [45] Jascha Sohl-Dickstein, Eric Weiss, Niru Maheswaranathan, and Surya Ganguli. Deep unsupervised learning using nonequilibrium thermodynamics. In *ICML*, 2015. 1
- [46] Jiaming Song, Chenlin Meng, and Stefano Ermon. Denoising diffusion implicit models. In *ICLR*, 2021. 5
- [47] Gerald Tesauro, Rajarshi Das, Hoi Chan, Jeffrey Kephart, David Levine, Freeman Rawson, and Charles Lefurgy. Managing power consumption and performance of computing systems using reinforcement learning. In *NeurIPS*, 2007. 3
- [48] Zhengzhong Tu, Hossein Talebi, Han Zhang, Feng Yang, Peyman Milanfar, Alan Bovik, and Yinxiao Li. Maxvit: Multi-axis vision transformer. In *ECCV*, 2022. 3
- [49] Kristof Van Moffaert and Ann Nowé. Multi-objective reinforcement learning using sets of pareto dominating policies. *JMLR*, 15(1):3483–3512, 2014. 2
- [50] Ashish Vaswani, Noam Shazeer, Niki Parmar, Jakob Uszkoreit, Llion Jones, Aidan N Gomez, Łukasz Kaiser, and Illia Polosukhin. Attention is all you need. In *NeurIPS*, 2017. 5
- [51] Jiazheng Xu, Xiao Liu, Yuchen Wu, Yuxuan Tong, Qinkai Li, Ming Ding, Jie Tang, and Yuxiao Dong. Imagereward: Learning and evaluating human preferences for text-to-image generation. In *NeurIPS*, 2023. 2, 3
- [52] Zhenqiang Ying, Haoran Niu, Praful Gupta, Dhruv Mahajan, Deepti Ghadiyaram, and Alan Bovik. From patches to pictures (paq-2-piq): Mapping the perceptual space of picture quality. In *CVPR*, 2020. 3
- [53] Jiahui Yu, Yuanzhong Xu, Jing Yu Koh, Thang Luong, Gungjan Baid, Zirui Wang, Vijay Vasudevan, Alexander Ku, Yinfei Yang, Burcu Karagol Ayan, Ben Hutchinson, Wei Han, Zarana Parekh, Xin Li, Han Zhang, Jason Baldridge, and Yonghui Wu. Scaling autoregressive models for content-rich text-to-image generation. *Transactions on Machine Learning Research*, 2022. 6, 7, 1
- [54] Lijun Yu, Yong Cheng, Kihyuk Sohn, José Lezama, Han Zhang, Huiwen Chang, Alexander G Hauptmann, Ming-Hsuan Yang, Yuan Hao, Irfan Essa, et al. Magvit: Masked generative video transformer. In *CVPR*, 2023. 2
- [55] Yufan Zhou, Bingchen Liu, Yizhe Zhu, Xiao Yang, Changyou Chen, and Jinhui Xu. Shifted diffusion for text-to-image generation. In *CVPR*, 2023. 1

Parrot: Pareto-optimal Multi-Reward Reinforcement Learning Framework for Text-to-Image Generation

Supplementary Material

This supplementary material provides:

- Sec. **A**: implementation details, including the training details, and details of quantitative experiments.
- Sec. **B**: more ablation studies on better tradeoff for different rewards.
- Sec. **C**: more ablation studies on original prompt guidance and training scheme of Parrot.
- Sec. **D**: more visual examples to show the advancements of Parrot.

A. Implementation Details

Training Details. We conduct our experiments with Jax implementation of Stable Diffusion 1.5 [38]. In terms of diffusion-based RL, we sample 256 images per RL-tuning iteration. For policy gradient updates, we accumulate gradients across all denoising timesteps. Our experiments employ a small range of gradient clip 10^{-4} . We keep negative prompt as null text.

Details of Quantitative Experiments. From Parti [53] prompts, we generate images of dimensions 512×512 . In all experiments in the main paper, we apply reward-specific preference expressed as “ $\langle \text{Reward } 1 \rangle, \langle \text{Reward } 2 \rangle, \langle \text{Reward } 3 \rangle, \langle \text{Reward } 4 \rangle$ ”, which is optional to select one or several rewards. Reward models are aesthetics, human preference, text-image alignment and image sentiment. During the inference stage, the guidance scale is also set as 5.0 for the diffusion sampling process. We employ the AdamW [22] as optimizer with $\beta_1 = 0.9$, $\beta_2 = 0.999$ and a weight decay of 0.1.

B. Better Tradeoff for Different Rewards

To verify that Parrot achieved better tradeoff for different rewards, we generate 1000 images from common animal dataset [4], where each text prompt consists of the name of a common animal. As shown in Fig. 9, using only text-image alignment with reward-specific preference “ $\langle \text{Reward } 3 \rangle$ ” yields images with higher text-image alignment score, while using only aesthetic model with reward-specific preference “ $\langle \text{Reward } 1 \rangle$ ” yields images with higher aesthetic score. In the case of using two reward-specific preferences “ $\langle \text{Reward } 1 \rangle, \langle \text{Reward } 3 \rangle$ ”, we observe that scores are balanced and show that better results across multiple rewards compared with Parrot without Pareto optimal selection.

C. Prompt Guidance and Training Scheme

Original Prompt Guidance. In Fig. 10, we provide additional ablation study of original prompt centered guidance

by adjusting the guidance scale w_1 and w_2 , which determines visual changes from original prompt and expanded prompt, respectively. We assigned 5 to both w_1 and w_2 in most of our experiments, which shows better text-image alignment performance in Fig. 10.

Ablation Study on Training Scheme. Fig. 11 provides ablation study comparing variation of the Parrot: Stable Diffusion, the prompt expansion network (PEN) tuning only, T2I model fine-tuning only, Parrot without joint optimization, and Parrot. In the second column, without fine-tuning the T2I diffusion model does not lead to significant improvements in terms of texture and composition. Furthermore, the third column demonstrates that fine-tuning the diffusion model enhances texture and perspective, yet this improvement is hindered by the limited information in the text prompt. We also observe that the quality of images from joint optimization surpasses that of combining decoupled generative models.

D. More Visual Examples

We show additional visual examples of Parrot in Figs. 12 to 17. Note that generated images from Parrot are improved across multiple-criteria. Fig. 12 highlights examples where the Parrot brings improvements in aesthetics. For example, Parrot effectively addresses issues such as poor cropping in the fourth column and improves color in the fifth column. Fig. 13 presents examples of images with improved human preference score generated by Parrot. In Fig. 14, we provide examples of improved text-image alignment achieved by Parrot. Fig. 15 shows examples where Parrot enhances image sentiment, producing emotionally rich images.

Finally, additional comparison results between diffusion-based RL baselines are described in Fig. 16, and Fig. 17. Diffusion-based RL baselines are listed: Stable Diffusion 1.5 [38], DPOK [10] with weighted sum of multiple reward scores, Promptist [9], Parrot without prompt expansion, and Parrot. For Parrot without prompt expansion, we only take original prompt as input.

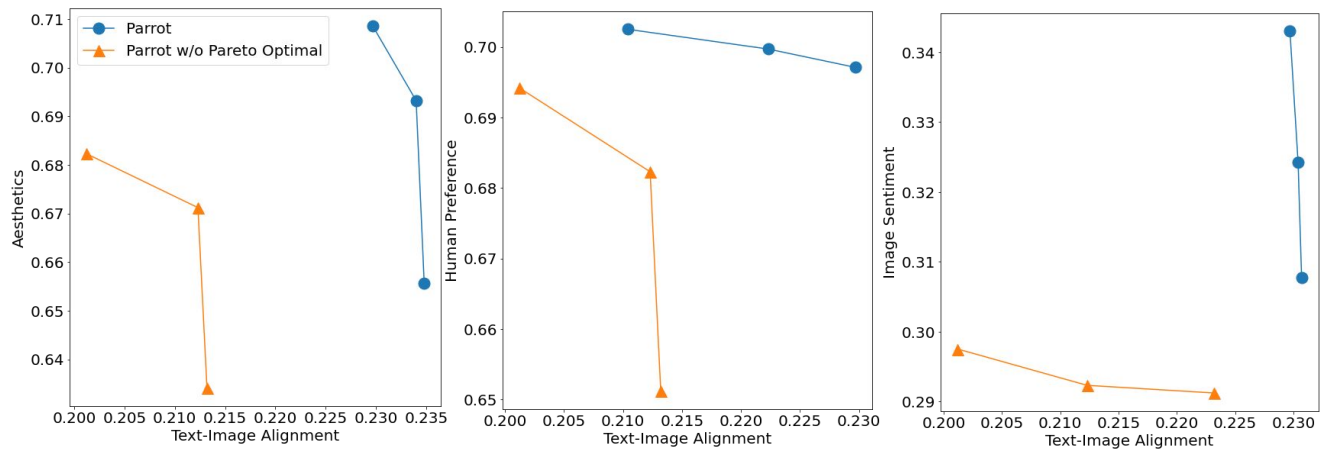


Figure 9. Comparing Parrot with/without Pareto Optimal. When we apply Pareto-optimal selection, we observe that each reward score increases based on reward-specific preference.

"Oil painting of a deer" → "Oil painting of a deer in a forest. the deer is standing in the middle of the painting, and the forest is behind it. The deer is brown, and the forest is green. the painting is done in a realistic style, and the texture is smooth. the atmosphere of the painting is peaceful and serene."

"A teapot" → "a teapot with a textured surface and a warm atmosphere."

"A parrot" → "A parrot with a green and blue body and a yellow beak. The parrot is sitting on a branch. The background is a blue sky with white clouds."

"A clock" → "A clock with a wooden frame and a white face. The clock is sitting in a room with a white wall. The room is lit by a single light bulb"

"A robot cooking" → "A robot is cooking in a kitchen. The robot has a chef's hat on. The kitchen is clean and well-organized. The robot is cooking a meal for a family of four. The meal is a roast chicken, potatoes, and green beans. The robot is carefully preparing the meal and takes pride in its work."



Figure 10. Original prompt centered guidance. We present visual comparison of 5 different pairs of w_1 and w_2 to demonstrate the effectiveness of guidance scales. For all experiments, we assign $w_1 = 5$ and $w_2 = 5$ (3rd row) for the best performance.

SD 1.5

PEN Tuning Only

T2I Model Tuning Only

Parrot w/o Joint Optimization

Parrot



A tree



A tree with a beautiful sky and clouds



A tree



A tree with a beautiful sky



A tree with a beautiful sky and clouds



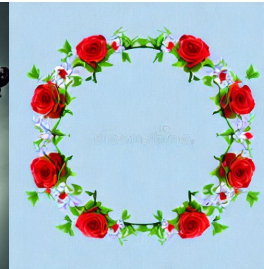
A crown



3d render of a golden crown with a red jewel on a white background.



A crown



A crown of flowers on a white background. The flowers are arranged in a circle and the crown is topped with a red rose. The background is a light blue color and the flowers are a variety of colors. The image is both beautiful and elegant.



3d render of a golden crown with a red jewel on a white background.



The city of London



The city of London at night with a beautiful view of the city lights.



The city of London



The city of London is a beautiful city with a rich history. The city is also known for its vibrant nightlife.



The city of London at night with a beautiful view of the city lights.



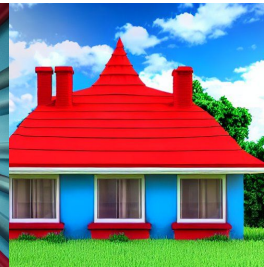
A cartoon house with red roof



3d render of a cartoon house with a red roof and a blue sky



A cartoon house with red roof



A cartoon house with a red roof and a blue sky



3d render of a cartoon house with a red roof and a blue sky

Figure 11. Visual examples of **Parrot** under different settings. From left to right, we provide results of Stable Diffusion 1.5 [38], the only fine-tuned PEN, the only fine-tuned T2I diffusion model, the **Parrot** without joint optimization, and the **Parrot**.



Figure 12. More Examples of aesthetics improvement from the **Parrot**. Given the text prompt, we generate images with Stable Diffusion and **Parrot**. After fine-tuning, the **Parrot** alleviates quality issues such as poor composition (e.g. bad cropping), misalignment with the user input (e.g. missing objects), or generally less aesthetic pleasing.



Figure 13. More Examples of human preference improvement from the **Parrot**. Given the text prompt, we generate images with Stable Diffusion 1.5 [38] and **Parrot**.



Figure 14. More examples of text-image alignment improvement from the **Parrot**. Given the text prompt, we generate images with the Stable Diffusion 1.5 [38] and the **Parrot**.

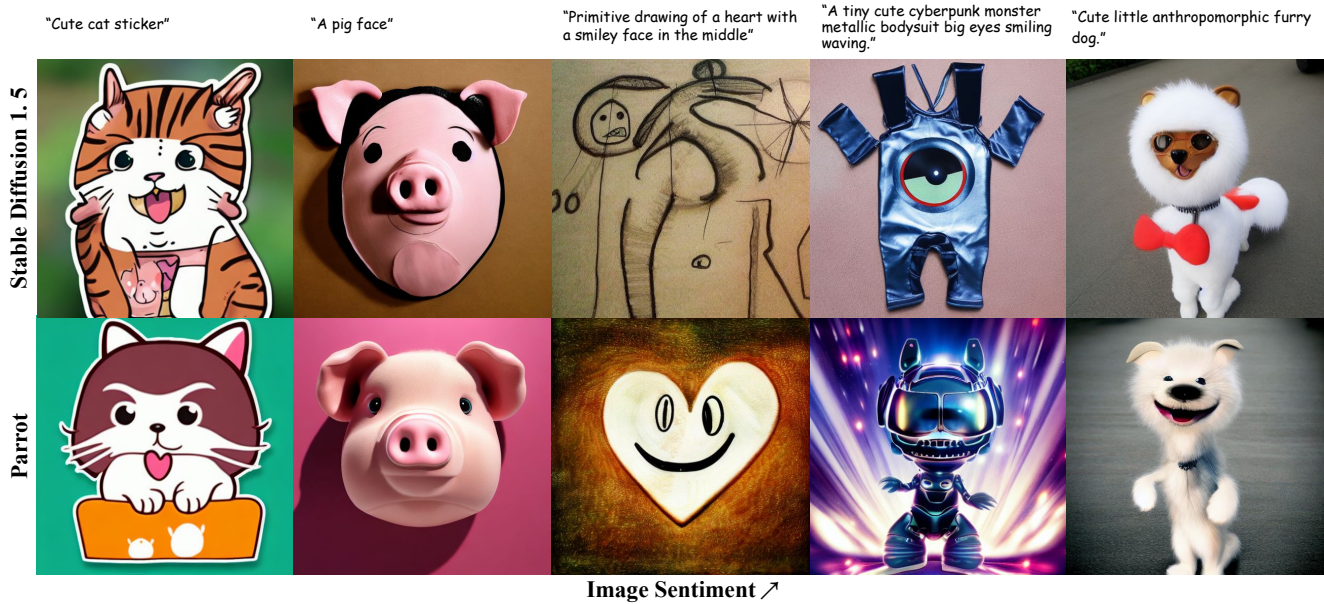


Figure 15. More examples of image sentiment improvement from the **Parrot**. Given the text prompt, we generate images with the Stable Diffusion 1.5 [38] and the **Parrot**.

SD 1.5

DPOK

Promptist

Parrot w/o PE

Parrot



Abstract cityscape

geometric

Abstract cityscape

geometric

Abstract geometric cityscape, hyperdetailed, artstation, cgsociety, 8k

Abstract cityscape

geometric

Abstract geometric cityscape with a beautiful sunset.



A painting of the city of nuremberg by john blanche

A painting of the city of nuremberg by john blanche

A painting of the city of nuremberg by john blanche, trending on artstation

A painting of the city of nuremberg by john blanche

A painting of the city of nuremberg by john blanche in a realistic style with a lot of detail and a warm color palette



A mix of paris and favelas.

A mix of paris and favelas.

A mix of paris and favelas, highly detailed, digital painting, artstation, concept art, sharp focus, illustration, art by greg rutkowski and alphonse mucha

A mix of paris and favelas.

A mix of paris and favelas, a beautiful city with a lot of colors.



A large magical beast called an owlbear

A large magical beast called an owlbear

A large magical beast called an owlbear, highly detailed, digital painting, artstation, concept art, sharp focus, illustration, art by greg rutkowski and alphonse mucha

A large magical beast called an owlbear

A large magical beast called an owlbear in the sunset

Figure 16. More results from the **Parrot** and baselines: Stable Diffusion 1.5 [38], DPOK [10] with weighted sum, Promptist [9], Parrot without prompt expansion, and Parrot.

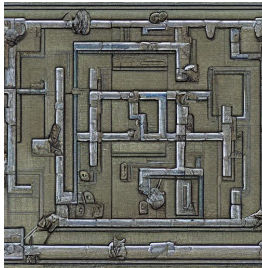
SD 1.5

DPOK

Promptist

Parrot w/o PE

Parrot



A dungeon labyrinth

A dungeon labyrinth

A dungeon labyrinth, RPG Reference, Oil Painting, Trending on Artstation, octane render, Insanely Detailed, 8K, HD

A dungeon labyrinth

A dungeon labyrinth with a dark and mysterious atmosphere



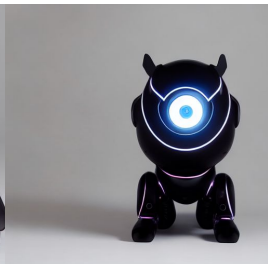
A red carpet floor

A red carpet floor

A red carpet floor, a fantasy digital painting by Greg Rutkowski and James Gurney, trending on Artstation, highly detailed

A red carpet floor

A red carpet floor with a beautiful floral pattern and a chandelier hanging from the ceiling.



Studio photo of a futuristic cute robot

Studio photo of a futuristic cute robot with a blue and white light.



A tree house in the jungle

A tree house in the jungle

A tree house in the jungle, highly detailed, digital painting, artstation, concept art, sharp focus, illustration, art by greg rutkowski and alphonse mucha

A tree house in the jungle

A tree house in the jungle with a beautiful view of the mountains

Figure 17. More results from the **Parrot** and baselines: Stable Diffusion 1.5 [38], DPOK [10] with weighted sum, Promptist [9], Parrot without prompt expansion, and Parrot.